Quantum Dynamics of a Photochemical Bond Cleavage Influenced by the Solvent Environment – a Dynamic Continuum Approach

Supporting Information

Sebastian Thallmair,[†,‡] Markus Kowalewski,[†,¶] Julius P. P. Zauleck,[†] Matthias K. Roos,[†] and Regina de Vivie-Riedle[*,†]

Department Chemie, Ludwig-Maximilians-Universität München, D-81377 München, Germany, and Lehrstuhl für BioMolekulare Optik, Ludwig-Maximilians-Universität München, D-80538 München, Germany

E-mail: regina.de_vivie@cup.uni-muenchen.de

[*]To whom correspondence should be addressed

[†]Department Chemie, Ludwig-Maximilians-Universität München, D-81377 München, Germany

[‡]Lehrstuhl für BioMolekulare Optik, Ludwig-Maximilians-Universität München, D-80538 München, Germany

[¶]Current adress: Department of Chemistry, University of California, Irvine, California 92697-2025, USA

ONIOM potential energy surface of the ground state of $Ph_2CH{-}PPh_3^+$

The potential energy surfaces (PESs) of diphenylmethyltriphenylphosphonium ions ($Ph_2CH{-}PPh_3^+$) are calculated at the ONIOM (CASSCF(10,10) / M06-2X / 6-31G(d)) level of theory. The high-level system $PhCH_2{-}PH_2Ph^+$ contains the thicker drawn part of the molecule in Fig. 1 in the manuscript and was shown to be a apropriate to model the excitations in $Ph_2CH{-}PPh_3^+$.[1] The thinner drawn phenyl rings are only contained in the low-level system $Ph_2CH{-}PPh_3^+$. They are replaced by H atoms[2] in the high-level system. According to reference 1, the active space of the complete active space self consisted field (CASSCF) calculations contains 4 π molecular orbitals (MOs) of each phenyl ring (2 bonding and 2 anti-bonding) and the σ and σ^* MOs of the C1-P bond. Fig. S1 shows the PES of the ground state of $Ph_2CH{-}PPh_3^+$. The minimum is located at a C1-P distance of $r = 1.9\,\text{Å}$ and a P-C1-X angle of $\phi = 125°$; the conical intersection (CoIn) at $r = 2.9\,\text{Å}$ and $\phi = 75°$.

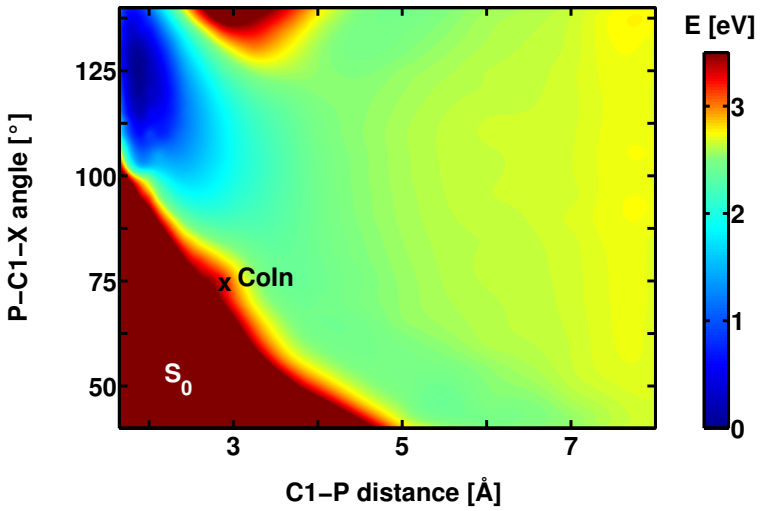

Figure S1: Two-dimensional potential energy surface of the ground state S_0 of $Ph_2CH{-}PPh_3^+$ calculated at the ONIOM (CASSCF(10,10) / M06-2X / 6-31G(d)) level of theory.

Quantum dynamics

The quantum dynamics were performed on a regular space grid. The time evolution of the system was calculated by solving the time-dependent Schrödinger equation numerically with the Chebychev propagation scheme.[3] The vibrational ground state eigenfunction $v = 0$ of the electronic ground state was determined propagating in imaginary time.[4] To express the kinetic operator $\hat{T}$ in the chosen two-dimensional coordinate space, the G-matrix method was used:[5–8]

$$\hat{T} = -\frac{1}{2}\sum_{r=1}^{M}\sum_{s=1}^{M}\frac{\partial}{\partial q_r}\left[G_{rs}\frac{\partial}{\partial q_s}\right] \tag{1}$$

$$\text{with} \quad G_{rs} = \sum_{i=1}^{3N}\frac{1}{m_i}\frac{\partial q_r}{\partial x_i}\frac{\partial q_s}{\partial x_i} \ . \tag{2}$$

It allows the use of arbitrary orthogonal coordinates for the quantum dynamical propagations. For details about the G-matrix elements see the following section.

The grid size, the number of grid points and the time step used for the different simulations are given in table S1. For the simulation including the non-adiabatic coupling matrix elements (NACME) a different grid size and a different number of grid points was used to have a better resolution of the NACME. The calculated effective radius is $R_{\text{eff}} = 4.17\,\text{Å}$ and the dynamic viscosity of acetonitrile at 25°C is $\eta = 0.343\,\text{mPa s}$.

Table S1: Size of the spatial grid, number of grid points and time step used for the different quantum dynamical simulations.

	r_{min} [Å]	r_{max} [Å]	ϕ_{min} [°]	ϕ_{max} [°]	N_r	N_ϕ	dt [au]
w/o dynamic continuum ansatz	1.65	8.00	40.0	140	2048	1024	200
w dynamic continuum ansatz	1.65	6.00	40.0	140	1024	512	2.0
w NACME	2.30	7.00	40.0	120	1024	1024	0.2

G-matrix elements

The G-matrix performs the coordinate transformation from cartesian to internal coordinates and therefore contains the derivatives of the internal coordinates q_r with respect to the cartesian coordinates x_i (for details see references 5 and 6). Due to practical reasons the G-matrix is calculated via its inverse:[7,8]

$$G_{rs}^{-1} = \sum_{i=1}^{3N} m_i \frac{\partial x_i}{\partial q_r} \frac{\partial x_i}{\partial q_s} \ . \tag{3}$$

Figure S2 shows the shape of the individual elements of G_{rs} used in our quantum dynamical simulations.

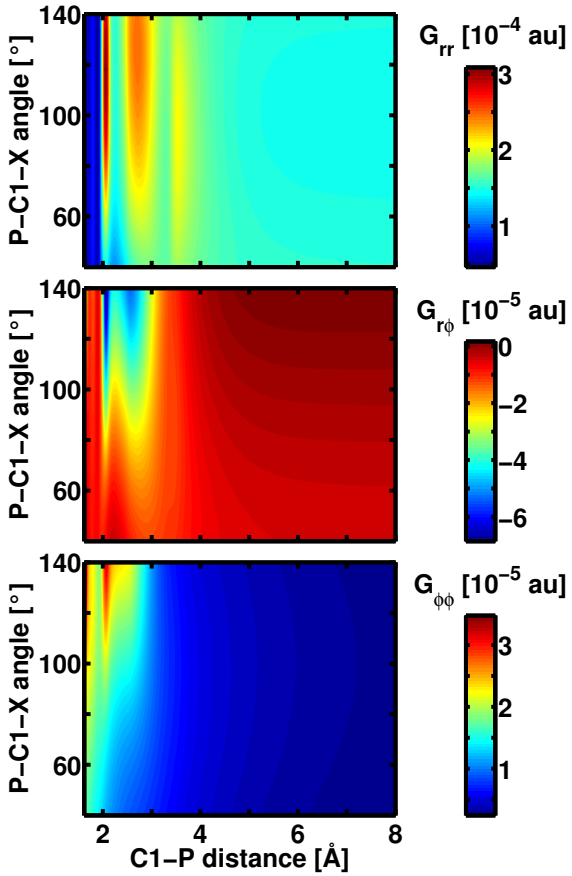

Figure S2: Two-dimensional G-matrix elements used for the quantum dynamics of $Ph_2CH{-}PPh_3^+$. The diagonal element G_{rr} is shown on top; the off-diagonal element $G_{r\phi}$ in the middle and the second diagonal element $G_{\phi\phi}$ at the bottom. The other off-diagonal element $G_{\phi r}$ is identical to $G_{r\phi}$ as the G-matrix is symmetric.

Potential energy of the critical points on the MS-CASPT2 level of theory

The effect of the dynamic electron correlation on the vertical excitation energy, the barrier in the S_1 state, the energy of the CoIn and potential energy in the dissociation limit calculated at the MS-CASPT2 level of theory is listed in table S2. The vertical excitation energy as well as the barrier height in the first excited state decrease. For the energy of the CoIn the decrease is less pronounced; the potential energy in the dissociation limit increases slightly.

As the changes of the vertical excitation energy and the barrier height are more decisive, they will affect the dynamics stronger than the changes at the other critical points. The decrease of the excitation energy will lead to a slower wave packet as the potential energy which is converted into kinetic energy is less. The time needed for the bond cleavage will increase. But the decreased barrier height has the opposite effect; the necessary time will decrease. Both effects will partly compensate each other. Quantum dynamics simulations with different initial momenta along the dissociation coordinate r additionally showed that the population in the S_0 state increases if the wave packet is slower. Thus an improvement of the description of the high-level system from the CASSCF to the MS-CASPT2 level of

Table S2: Comparison of CASSCF(10,10) and MS-CASPT2 energies for the high-level system (second and third column) and of the ONIOM energies for the complete precursor $Ph_2CH{-}PPh_3^+$ (fourth and fifth column) where the high-level system is calculated at the CASSCF(10,10) and MS-CASPT2 level of theory respectively. The S_0 minimum is always set to 0.0 eV.

	E_{CAS} [eV]	E_{CASPT2} [eV]	$E_{\mathrm{CAS/M06-2X}}$ [eV]	$E_{\mathrm{CASPT2/M06-2X}}$ [eV]
S_0 minimum	0.0	0.0	0.0	0.0
$S_0 \rightarrow S_1$	5.99	5.22	5.99	5.22
S_1barrier	6.39	5.56	6.36	5.53
$\Delta E_{\mathrm{barrier}}$	0.403	0.331	0.375	0.302
S_1 / S_0 CoIn	4.00	3.88	3.30	3.18
dissociation limit	4.06	4.14	3.78	3.85

theory will only slightly affect the simulated reaction time and product yield. The observed reaction mechanism will remain unchanged.

Optimized geometries

In the following the optimized geometry of the ground state minimum of $Ph_2CH{-}PPh_3^+$ (DFT, B3LYP / 6-31g(d)) and the structure with the minimal energy difference between S_1 and S_0 at the ONIOM level of theory, where the S_1/S_0 CoIn is located, are given in xyz-format (all coordinates are given in Å):

S_0 minimum of $Ph_2CH-PPh_3^+$							
C	-0.857563	-0.363243	2.740120	C	-3.904048	1.193641	-1.825089
C	-0.857563	-0.363243	4.136624	C	-4.758800	0.209656	-1.326982
C	-0.857563	0.841154	4.841799	C	-4.361545	-0.552605	-0.227744
C	-0.856673	2.048881	4.142127	C	-3.115493	-0.342429	0.364361
C	-0.851032	2.049395	2.747461	H	-2.013596	2.184599	-1.623796
C	-0.853155	0.846224	2.026641	H	-4.209166	1.808742	-2.666574
C	-0.880912	0.923931	0.505055	H	-5.732204	0.049228	-1.780938
P	0.553877	-0.001046	-0.330103	H	-5.027687	-1.305911	0.182917
C	0.517185	0.439117	-2.096536	H	-2.843546	-0.924442	1.237017
C	0.599261	1.797043	-2.459860	C	-0.700253	-2.495806	-0.620834
C	0.592713	2.163352	-3.803077	C	-0.775043	-3.880705	-0.482911
C	0.506237	1.182728	-4.795959	C	0.270872	-4.586815	0.116795
C	0.437019	-0.164062	-4.442198	C	1.398748	-3.906729	0.577736
C	0.445454	-0.540090	-3.097451	C	1.485457	-2.520941	0.446454
H	-0.846940	-1.312929	2.215166	H	-1.519025	-1.963354	-1.091187
H	-0.859334	-1.308491	4.671702	H	-1.651438	-4.407711	-0.847813
H	-0.860511	0.838254	5.927692	H	0.207297	-5.665973	0.220175
H	-0.858520	2.992397	4.679905	H	2.216089	-4.452555	1.038998
H	-0.851139	2.996680	2.213670	H	2.367591	-2.003812	0.806828
H	-0.618846	1.954488	0.234810	C	2.399308	0.648467	1.716078
H	0.686844	2.570247	-1.701169	C	3.650060	1.051488	2.181513
H	0.658404	3.212488	-4.074981	C	4.669060	1.373368	1.283123
H	0.500526	1.470915	-5.842909	C	4.438939	1.285321	-0.090196
H	0.379884	-0.928828	-5.210685	C	3.191926	0.885547	-0.568494
H	0.401473	-1.591562	-2.837609	H	1.627922	0.392578	2.430697
C	-2.239750	0.631801	-0.138374	H	3.825451	1.112398	3.251277
C	0.433997	-1.804790	-0.150298	H	5.640696	1.687494	1.652754
C	2.156330	0.570647	0.331175	H	5.229081	1.526783	-0.794606
C	-2.658817	1.403261	-1.233867	H	3.031528	0.819900	-1.638206

S_1/S_0 CoIn of $Ph_2CH-PPh_3^+$							
C	0.294154	-1.602203	1.912734	C	-2.255969	-0.595800	-2.928832
C	0.621997	-1.826153	3.251610	C	-3.147218	-1.542878	-2.423208
C	1.007022	-0.763660	4.070578	C	-3.003787	-1.987426	-1.108301
C	1.063701	0.527240	3.542836	C	-1.971752	-1.498803	-0.306080
C	0.741769	0.750568	2.204326	H	-0.550484	0.641117	-2.531738
C	0.351269	-0.307908	1.371052	H	-2.368740	-0.225073	-3.943419
C	0.000000	0.000000	0.000000	H	-3.955918	-1.919045	-3.042749
P	2.819669	-0.677408	0.024219	H	-3.705104	-2.707433	-0.696474
C	2.782977	-0.237245	-1.742214	H	-1.901171	-1.834719	0.721734
C	2.865053	1.120681	-2.105538	C	1.565539	-3.172168	-0.266512
C	2.858505	1.486990	-3.448755	C	1.490749	-4.557067	-0.128589
C	2.772029	0.506366	-4.441637	C	2.536664	-5.263177	0.471117
C	2.702811	-0.840424	-4.087876	C	3.664540	-4.583091	0.932058
C	2.711246	-1.216452	-2.743129	C	3.751249	-3.197303	0.800776
H	0.007998	-2.446541	1.294024	H	0.746767	-2.639716	-0.736865
H	0.573669	-2.834330	3.652918	H	0.614354	-5.084073	-0.493491
H	1.258603	-0.940196	5.112078	H	2.473089	-6.342335	0.574497
H	1.360123	1.362210	4.170841	H	4.481881	-5.128917	1.393320
H	0.788979	1.760803	1.804978	H	4.633383	-2.680174	1.161150
H	0.355952	0.978807	-0.344955	C	4.665100	-0.027895	2.070400
H	2.952636	1.893885	-1.346847	C	5.915852	0.375126	2.535835
H	2.924196	2.536126	-3.720659	C	6.934852	0.697006	1.637445
H	2.766318	0.794553	-5.488587	C	6.704731	0.608959	0.264126
H	2.645676	-1.605190	-4.856363	C	5.457718	0.209185	-0.214172
H	2.667265	-2.267924	-2.483287	H	3.893714	-0.283784	2.785019
C	-1.058458	-0.559590	-0.808639	H	6.091243	0.436036	3.605599
C	2.699789	-2.481152	0.204024	H	7.906488	1.011132	2.007076
C	4.422122	-0.105715	0.685497	H	7.494873	0.850421	-0.440284
C	-1.224458	-0.108012	-2.127500	H	5.297320	0.143538	-1.283884

Complete references (27) and (30) from the manuscript

(27) Frisch, M. J., Trucks, G. W., Schlegel, H. B., Scuseria, G. E., Robb, M. A., Cheeseman, J. R., Scalmani, G., Barone, V., Mennucci, B., Petersson, G. A., Nakatsuji, H., Caricato, M., Li, X., Hratchian, H. P., Izmaylov, A. F., Bloino, J., Zheng, G., Sonnenberg, J. L., Hada, M., Ehara, M., Toyota, K., Fukuda, R., Hasegawa, J., Ishida, M., Nakajima, T., Honda, Y., Kitao, O., Nakai, H., Vreven, T., J. A. Montgomery, Jr., Peralta, J. E., Ogliaro, F., Bearpark, M., Heyd, J. J., Brothers, E., Kudin, K. N., Staroverov, V. N., Kobayashi, R., Normand, J., Raghavachari, K., Rendell, A., Burant, J. C., Iyengar, S. S., Tomasi, J., Cossi, M., Rega, N., Millam, J. M., Klene, M., Knox, J. E., Cross, J. B., Bakken, V., Adamo, C., Jaramillo, J., Gomperts, R., Stratmann, R. E., Yazyev, O., Austin, A. J., Cammi, R., Pomelli, C., Ochterski, J. W., Martin, R. L., Morokuma, K., Zakrzewski, V. G., Voth, G. A., Salvador, P., Dannenberg, J. J., Dapprich, S., Daniels, A. D., Farkas, O., Foresman, J. B., Ortiz, J. V., Cioslowski, J., and Fox, D. J., *Gaussian 09, Revision A.02, Inc.*, Wallingford C, 2009.

(30) Werner, H.-J., Knowles, P. J., Knizia, G., Manby, F. R., Schütz, M., Celani, P., Korona, T., Lindh, R., Mitrushenkov, A., Rauhut, G., Shamasundar, K. R., Adler, T. B., Amos, R. D., Bernhardsson, A., Berning, A., Cooper, D. L., Deegan, M. J. O., Dobbyn, A. J., Eckert, F., Goll, E., Hampel, C., Hesselmann, A., Hetzer, G., Hrenar, T., Jansen, G., Köppl, C., Liu, Y., Lloyd, A. W., Mata, R. A., May, A. J., McNicholas, S. J., Meyer, W., Mura, M. E., Nicklass, A., O'Neill, D. P., Palmieri, P., Peng, D., Pflüger, K., Pitzer, R., Reiher, M., Shiozaki, T., Stoll, H., Stone, A. J., Tarroni, R., Thorsteinsson, T., and Wang, M., *MOLPRO, version 2012.1, a package of ab initio programs*, 2012.

References

(1) Thallmair, S.; Fingerhut, B. P.; de Vivie-Riedle, R. Ground and Excited State Surfaces for the Photochemical Bond Cleavage in Phenylmethylphenylphosphonium Ions. *J. Phys. Chem. A* **2013**, *117*, 10626–10633.

(2) Dapprich, S.; Komáromi, I.; Byun, K.; Morokuma, K.; Frisch, M. J. A New ONIOM Implementation in Gaussian98. Part I. The Calculation of Energies, Gradients, Vibrational Frequencies and Electric Field Derivatives. *J. Mol. Struct.: THEOCHEM* **1999**, *461–462*, 1–21.

(3) Tal-Ezer, H.; Kosloff, R. An Accurate and Efficient Scheme for Propagating the Time Dependent Schrödinger Equation. *J. Chem. Phys.* **1984**, *81*, 3967–3971.

(4) Kosloff, R.; Tal-Ezer, H. A Direct Relaxation Method for Calculating Eigenfunctions and Eigenvalues of the Schrödinger Equation on a Grid. *Chem. Phys. Lett.* **1986**, *127*, 223–230.

(5) Wilson Jr., E. B.; Decius, J. C.; Cross, P. C. *Molecular Vibrations*; McGraw-Hill: New York, 1955.

(6) Schaad, L.; Hu, J. The Schrödinger Equation in Generalized Coordinates. *J. Mol. Struct.: THEOCHEM* **1989**, *185*, 203–215.

(7) Alexandrov, V.; Smith, D. M. A.; Rostkowska, H.; Nowak, M. J.; Adamowicz, L.; McCarthy, W. Theoretical Study of the O-H Stretching Band in 3-Hydroxy-2-methyl-4-pyrone. *J. Chem. Phys.* **1998**, *108*, 9685–9693.

(8) Kowalewski, M.; Mikosch, J.; Wester, R.; de Vivie-Riedle, R. Nucleophilic Substitution Dynamics: Comparing Wave Packet Calculations with Experiment. *J. Phys. Chem. A* **2014**, *118*, 4661–4669.